PHYS. MED. BIOL., 1976, VOL. 21, NO. 3, 390–398. © 1976

Beam Hardening in X-ray Reconstructive Tomography

RODNEY A. BROOKS, PH.D. and GIOVANNI DI CHIRO, M.D.†

Section on Neuroradiology, National Institute of Neurological and Communicative Disorders and Stroke, Bethesda, MD 20014, U.S.A.

Received 25 *April* 1975, *in final form* 10 *October* 1975

ABSTRACT. As a polychromatic X-ray beam passes through matter, low energy photons are preferentially absorbed, and the (logarithmic) attenuation is no longer a linear function of absorber thickness. This leads to various artifacts in reconstructive tomography. If a water bag is used, the nonlinear attenuation in bone causes a distortion of the bone values and a spill-over inside the skull, or 'pseudo-cortex' artifact. If no water bag is used, there is an additional effect due to the varying thickness of soft tissue which causes a depression of interior values, or 'cupping'. Both artifacts can be remedied by additional prefiltering of the beam and by applying a linearization correction to the detector outputs.

1. Introduction

Since the introduction of the EMI scanner in 1972 (Hounsfield 1972, 1973, Ambrose 1973), there has been a flurry of interest in reconstructive X-ray transmission tomography, with at least a dozen companies now offering, or about to offer, devices for computerized axial tomography (CAT). One of the questions which has been raised in the literature is the effect of heterogeneity of the X-ray beam (Cho 1974, McCullough, Baker, Houser and Reese 1974, Shepp and Logan 1974).

Since all substances attenuate low-energy X-rays more strongly than high-energy ones, primarily because of photoelectric absorption, a heterogeneous beam traversing an absorbing medium becomes proportionately richer in high-energy photons, and hence more penetrating, or 'harder'. Hence the attenuation produced by a given material, defined as the negative logarithm of the ratio of transmitted to incident intensities, is not strictly proportional to its thickness. In other words, Beer's law does not apply to a heterogeneous beam. The result is that the projections are distorted, a projection being a plot of attenuation against beam position as the beam scans linearly across the object.

The problem can be approached by resolving the total beam intensity I into its energy spectrum (McCullough *et al.* 1974):

$$I = \int I(E)\,\mathrm{d}E \tag{1}$$

where $I(E)$ is the beam intensity (energy flux density) per unit energy interval. Beer's law then applies at each energy:

$$I(E) = I_0(E)\exp\left(-\mu(E)\,x\right) \tag{2}$$

† Address for reprints: Dr Di Chiro, Section on Neuroradiology, National Institutes of Health, Building 10, Room 2D13, Bethesda, MD 20014, U.S.A.

where $I_0(E)$ is the incident energy flux density per unit energy interval, $\mu(E)$ is the linear attenuation coefficient for photons of energy E and x is the thickness of absorber.

The purpose of this study is to analyse the effects of beam hardening on the reconstructed tomogram. A computer simulation is used which enables us to concentrate on beam hardening and to exclude other distorting factors. First, beam hardening effects in bone are examined. Because of its high calcium content, photoelectric absorption in bone is high and the effects of beam hardening are emphasized.

A second effect occurs in CAT scanners which do not use a water bag (Ledley, Di Chiro, Luessenhop and Twigg 1974). The water bag, originally introduced by EMI Ltd (Hounsfield 1972), surrounds the head in such a manner that all X-rays traverse the same distance of tissue or water. Without a water bag, different rays traverse different tissue thicknesses, with the result that the projections are distorted because of beam hardening.

Finally, both situations are considered together, and the results applied to the human head, on which the overwhelming number of CAT studies have been performed, and where beam hardening effects first became apparent.

2. Bone (with water bag)

We consider beam hardening in bone, assuming that a scanner with water bag is used, and that soft tissue has the same attenuation coefficients as water. Thus, in the absence of bone, the total path length through water or equivalent is always the same (27 cm, see McCullough *et al.* 1974), and the effects of beam hardening are negligible.

In the presence of bone, the path length remains the same but the bone produces additional attenuation of the X-ray beam. This can be calculated using eqns (1) and (2) and attenuation coefficients compiled by Hubbell (1969). Beam intensities are expressed as energy flux density, rather than photon fluence rate, since this is what determines the detector signal. A continuous bremsstrahlung spectrum is assumed at the anode, with a peak energy of 120 keV, followed by a prefilter of 4·5 mm aluminium, as reported for the EMI scanner (McCullough *et al.* 1974). The 27 cm of water-equivalent is also treated as a prefilter. The additional attenuation when some water (tissue) is replaced by bone is then calculated and shown in fig. 1. The slope of the curve is initially described by $\mu_{\text{eff}} = 0{\cdot}244\ \text{cm}^{-1}$, corresponding to an effective energy of 71·6 keV, and then falls off because of beam hardening. This curve is compared with an 'ideal' curve which continues linearly with the same initial slope, and hence does not include the effects of beam hardening. Note that the non-linearity at 7 cm is 10·2%.

An accuracy check can be performed at this stage by making a similar calculation for a small additional amount of water placed in the beam. The initial slope for water is found to be $\mu_{\text{eff}} = 0{\cdot}191\ \text{cm}^{-1}$, which agrees remarkably well with the experimental values $0{\cdot}19\ \text{cm}^{-1}$ (Hounsfield 1973) and $0{\cdot}190\ \text{cm}^{-1}$ (McCullough *et al.* 1974) reported for the EMI scanner. The

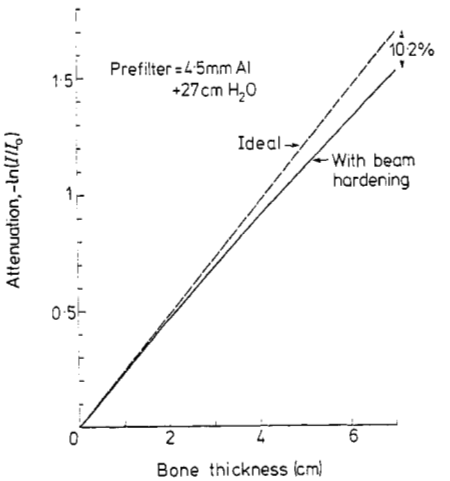

Fig. 1. Attenuation plotted against bone thickness. A water bag is used, with a total water–tissue path length of 27 cm. The bone thickness represents the amount of water which has been replaced with bone.

corresponding effective beam energy is 73.6 keV. Note, incidentally, that the effective beam energy is different for water and bone. This difference is not a consequence of calculational errors (although they may be present), but arises because the attenuation coefficients of the two substances have a different energy dependence. In fact, for some materials the difference in effective beam energy would be even larger.

The next step is to consider the effect of this non-linearity on the projections. We will treat two configurations of bone: a small circle, and a ring or annulus approximating the skull. The results are shown in fig. 2. In each case the

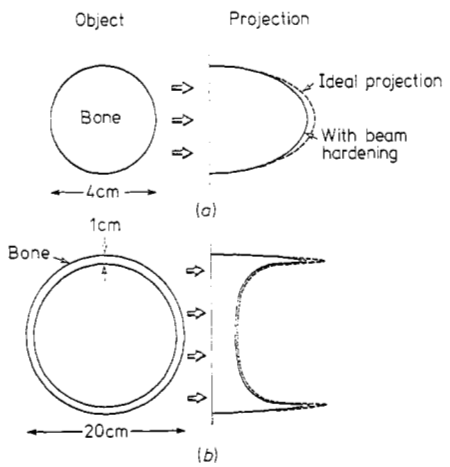

Fig. 2. Projections of (*a*) a 4 cm circle and (*b*) a 1 cm thick annulus of bone. A projection is defined as a plot of $-\ln(I/I_0)$ against position, and hence, ideally, is a linear function of bone thickness (dashed line). The actual projection (solid line) reflects the non-linear relation between attenuation and bone thickness shown in fig. 1.

projections are based on the calculated distance each ray travels in bone. The dashed lines show what the projections would be if the attenuation were a linear function of bone thickness (dashed curve of fig. 1), while the solid lines show how the projections are flattened because of beam hardening effects (solid curve of fig. 1). For the 4 cm circle the maximum distortion at the centre is 7%, while for the annulus the maximum distortion near the edge is 16%.

Finally, we turn to the reconstructed image which results from the distorted projections. The procedure for obtaining the reconstruction is summarized as follows: First, ideal projections are calculated, assuming (arbitrarily) an attenuation coefficient of 500 Hounsfield units† for the bone. These are then distorted, or flattened, according to the non-linear curve of fig. 1. Finally, reconstructions are made using the convolution method (Bracewell and Riddle 1967, Ramachandran and Lakshminarayanan 1971, Shepp and Logan 1974), which is used in most commercial CAT scanners.

A reconstruction of the bone ring, or skull, is shown in fig. 3. Note that the values near the skull are distorted by an artifact arising from the sharp edges, known as overshoot, ringing or the Gibbs' phenomenon (Bracewell 1965), which is responsible for the appearance of negative numbers and numbers greater than 500. (This artifact can be eliminated or reduced by the use of special filtering not incorporated in our reconstruction algorithm.) However, the artifact produces a ripple effect only, and does not shift average values over a large area. Thus, the following effects of beam hardening in bone can be distinguished.

The primary effect is to reduce the attenuation coefficient of the bone. If the average coefficient over a large bone area is compared with the nominal value of 500, the average reduction is found to be approximately 10%. In addition, there is a slight spill-over into the soft tissue region which is greatest near the inside edge of the skull, where the values are increased by about 3–5 Hounsfield units, although this is partially obscured by the Gibbs' phenomenon. In comparison, the statistical fluctuations in a typical scanner are $\sim \pm 2$ units. The elevated values in this area, indicated by dashed lines in fig. 3, were originally considered to represent the higher density grey matter of the cerebral cortex (Ambrose 1973), and are now recognized as an artifact (Gado and Phelps 1975, Hounsfield 1975), that is, a 'pseudo-cortex'. In the case of the 4 cm circle of bone (reconstruction not shown), the only noticeable effect is to reduce the bone attenuation coefficients as above.

When the reconstructions are made from ideal projections, these artifacts do not appear. The bone has values close to 500 Hounsfield units, and that of the soft tissue is 0, thus confirming that the distortion described above is due to beam hardening and not to the algorithm.

---

† Hounsfield units, or EMI numbers, are rapidly becoming the accepted means for describing attenuation coefficients in reconstructed tomograms. They are based on a scale in which air has the value −500 and water 0. Thus, five Hounsfield units correspond to a variation of 1% of the difference in attenuation coefficients between air and water at the energy of the radiation used (McCullough *et al.* 1974). (See also Note added in proof, p. 397).

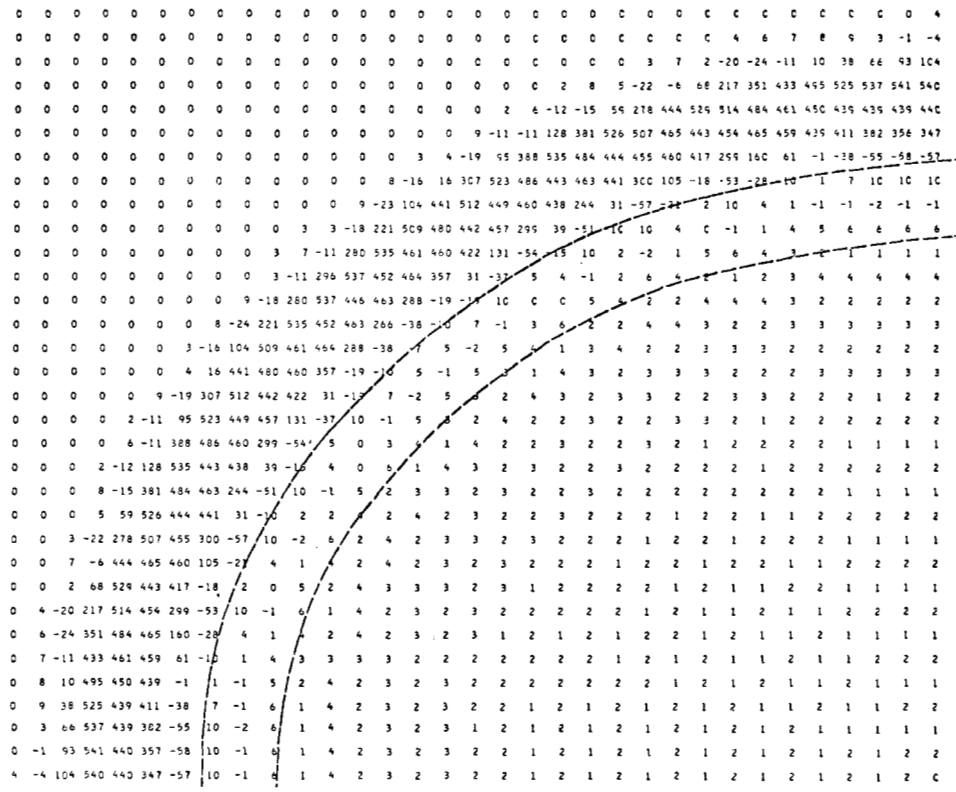

Fig. 3. Computer reconstruction of one quadrant of bone annulus (with water bag). Hounsfield's scale is used, with gas $= -500$ and water $= 0$, so that five units correspond to 1% of the attenuation coefficient of water. The area between the dashed lines shows how the beam hardening in bone produces a spill-over into the soft tissue region, responsible for the pseudo-cortex artifact.

The beam hardening error can easily be compensated by processing the detector output, before reconstruction, so as to correct for the non-linearity of fig. 1. Such a linearizing procedure has recently been introduced in the EMI scanner (Hounsfield 1975).

3. Soft tissue (no water bag)

If a water bag is not used, the path length through tissue-equivalent material varies, and this leads to additional beam-hardening errors. We will now neglect the presence of bone and consider a 20 cm circle of soft tissue with attenuation coefficients equal to those of water.

The calculation of attenuation against thickness is made as before. The resulting curve is similar to fig. 1, except that the non-linearity is not as great, the deviation for 20 cm of water being 9·2%. The effect of this non-linearity on the projections is once again to flatten them, in a manner similar to fig. 2(a).

A cross-section of the resulting reconstructed image is shown in fig. 4 (solid line), with the Gibbs' phenomenon averaged out. Note that the attenuation values are depressed from the nominal value of 0, with the depression greatest in the centre and least at the edges, producing a 'cupping' effect. If the

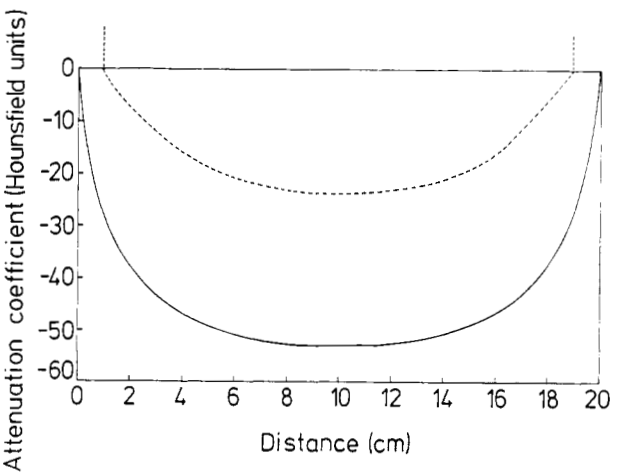

Fig. 4. Cross-sectional plots of reconstructed tomograms for circles of soft tissue (no water bag). Note the depression of values in the central area, referred to in the text as 'cupping'. The solid line represents a 20 cm circle of soft tissue, and the dashed line is for an 18 cm circle surrounded by a 1 cm thick annulus of bone. Note that in the latter case the cupping effect is reduced.

depression were constant, it could easily be calibrated out with a scale factor change; in fact, the variation from centre to edge is about 50 Hounsfield units. No attempt is made to compare these results with actual pictures from commercial scanners that omit the water bag (e.g. ACTA and DELTA scanners), since such effects would be obscured by corrective mechanisms, the details of which have not been made public.

In order to verify that the cupping effect is not caused by the algorithm, reconstructions were made from ideal projections. These reconstructions, as expected, show a uniform value of 0 throughout the circle. In fact, a comparison of figs 2(a) and 4 will convince the reader that the cupping is a direct outcome of beam-hardening. The point is that a depression of the central part of each projection (fig. 2(a)) naturally leads to a depression of the central part of the reconstructed image (fig. 4).

The cupping can be reduced by linearizing the detector output, as discussed in section 2. Another approach is to provide additional prefiltering to remove low-energy photons, leaving Compton scattering as the dominant attenuation mechanism. In this manner, the attenuation against thickness curve becomes more linear. For example, if a 3·5 cm aluminium prefilter is used, instead of 4·5 mm, the non-linearity is reduced to 1·5% for 20 cm of tissue. This reduces the cupping effect to a variation of about 15 Hounsfield units (reconstruction not shown).

While such a filter would remove 90% of the energy flux density, as compared with a 4·5 mm filter, it must be realized that the water bag also attenuates the beam. For example, for a head of average diameter 20 cm, the central rays pass through 7 cm of water, which removes 78% of the beam energy, and rays near the side are attenuated even more. Thus, the added attenuation due to the 3·5 cm prefilter is comparable to the average attenuation produced by the water bag, while the dose to the patient is actually reduced, since all the filtration occurs between the source and patient. High Z filters, such as copper, tin or Thoraeus filters, could produce even better results.

It should also be noted that, since prefiltering raises the effective beam energy, the relative attenuation coefficients of soft tissue will change slightly, and so the contrast of the reconstructed image will be altered. This effect, however, is minimal.

4. Bone and soft tissue (no water bag)

Finally, let us analyse the effect of beam hardening when both situations are present simultaneously, bone and no water bag. We will consider a head, as approximated by a 20 cm circle of tissue-equivalent material, surrounded by a 1 cm thick annulus of bone.

The calculations are performed as before, and the results are shown in fig. 4 (dashed line). Note that the two-beam hardening errors partially compensate, and the cupping effect is reduced. That is, for rays through the central region, the amount of bone is small and the amount of soft tissue greatest; for peripheral rays, the added distance in bone partially compensates for the reduced amount of soft tissue, so that the flattening referred to earlier is more constant throughout the projection. Even with minimal filtering (4·5 mm Al), the result is a variation of only 15 Hounsfield units (3%) from the centre of the brain to within a fraction of a cm of the skull. With a 3·5 cm Al prefilter, the cupping is virtually unnoticeable (reconstruction not shown).

Linearization of the detector output can also be used as a corrective measure, but the effects of bone and soft tissue cannot simultaneously be corrected. The best choice would be to linearize for soft tissue, as this is responsible for the greatest distortion. When bone is present, it will cause an additional flattening that will not be properly compensated; however, as we have seen, this will affect primarily the interior of the bone.

Alternatively, one could form a preliminary reconstruction of the image outline and correct for soft tissue hardening based on path lengths computed from the outline, with the bone correction applied subsequently as a linearization.

5. Summary

If a water bag is used, the beam hardening in bone lowers the apparent attenuation coefficient of the bone and also produces a pseudo-cortex artifact. If a water bag is not used, beam hardening in soft tissue produces a 'cupping' effect; i.e., a lowering of the attenuation coefficients, which is greater in the centre

than near the edge. For the case of the head, these two effects partially compensate and the cupping is reduced.

In both cases, the effects of beam hardening can be minimized by the use of additional prefiltering and/or linearization of the detector signal.

We would like to express our gratitude to Dr. William Kiker of the Armed Forces Radiobiology Institute for helpful discussions.

Note added in proof: Since the submission of this manuscript, EMI have introduced a new scale which is expanded by a factor of two. This scale is also used by Ohio Nuclear for their Delta scanner. All Hounsfield numbers in the present article should be multiplied by a factor of two in order to convert to the new scale.

Résumé

Durcissement des faisceaux dans la tomographie reconstructive des rayons X

Au passage d'un faisceau de rayons X polychromes, les photons à faible énergie sont absorbés préférentiellement et l'atténuation (logarithmique) n'est plus une fonction linéaire de l'épaisseur de la matière absorbante. Ceci conduit à différents artefacts dans la tomographie reconstructive. Si l'on se sert de vessies à eau, l'atténuation non-linéaire dans les os cause une distorsion des valeurs des os et un épanchement à l'intérieur du crâne, ou artefact 'pseudo-cortex'. Si l'on ne se sert pas de vessies à eau, il y a un effet additionnel dû à l'épaisseur variable des tissus mous, qui cause une dépression des valeurs intérieures on 'creux'. On peut remédier à ces deux artefacts par un filtrage préliminaire additionnel du faisceau et en appliquant une correction de linéarisation aux sorties du détecteur.

Zusammenfassung

Strahlenhärtung in rekonstruktiver Tomographie

Wenn ein polychromatischer Röntgenstrahl Materie durchdringt, werden vor allem Photonen mit niedriger Energie absorbiert, und die (logarithmische) Schwächung ist keine lineare Funktion der Absorberdicke mehr. Dies führt in der rekonstruktiven Tomographie zu verschiedenen Kunstprodukten. Bei Verwendung eines Wasserbeutels verursacht die nichtlineare Schwächung im Knochen eine Verzerrung der Knochenwerte und ein Spillover im Schädel oder 'Pseudokortex'-Kunstprodukt. Wenn kein Wasserbeutel verwendet wird, kommt ein Effekt hinzu, der auf die verschiedene Dicke des weichen Gewebes zurückzuführen ist und eine Senkung der inneren Werte oder 'Schröpfen' verursacht. Beiden Kunstprodukten kann man abhelfen, indem man den Strahl mit zusätzlichen Vorfiltern versieht und an den Detektorausgängen Linearisations-Korrektoren anbringt.

Резюме

Увеличение жесткости пучка в воспроизводящей томографии рентгеновских лучей

При прохождени полиэнергетического пучка рентгеновских лучей через вещество имеет место примущественное поглощение фотонов малой энергии, и ослабление (логарифмическое) больше не является линейной функцией толщины поглотителя. Это ведет к различным артефактам в воспроизводящей томографии. Если используется водяной мешок, то нелинейное ослабление в кости вызывает искажение в значениях и перекрытие внутри черепа или артефакт 'ложной коры головного мозга'. Если водяной мешок не используется, то из-за изменяюшейся толщины мягких тканей возникает дополнительный эффект, вызывающий подавление значений внутренней части ткани или 'вдавливание'. Оба эти артефакта можно исправить за счет дополнительной предварительной фильтрации луча и применения поправки на линеаризацию к выходным величинам детектора.

References

Ambrose, J., 1973, *Br. J. Radiol.*, **46**, 1023–1047.

Bracewell, R. N., 1965, *The Fourier Transform and Its Applications* (New York: McGraw-Hill) p. 209.

Bracewell, R. N., and Riddle, A. C., 1967, *Astrophys. J.*, **150**, 427–434.

Cho, Z. H., 1974, *IEEE Trans. Nucl. Sci.*, **NS-21**(3), 44–71.

Gado, M., and Phelps, M., 1975, *Radiology*, **117**, 71–74.

Hounsfield, G. N., 1972, *British Patent* No. 1283915 (British Patent Office, London).

Hounsfield, G. N., 1973, *Br. J. Radiol.* **46**, 1016–1022.

Hounsfield, G. N., 1975, in *Reconstructive Tomography in Diagnostic Radiology and Nuclear Medicine*, Ed. M. M. Ter-Pogossian (Baltimore University Park Press) in press.

Hubbell, J. H., 1969, *U.S. National Bureau of Standards* NSRD–NBS 39 (Washington: U.S. Government Printing Office).

Ledley, R. S., Di Chiro, G., Luessenhop, A. J., and Twigg, H. L., 1974, *Science, N.Y.*, **186**, 207–212.

McCullough, E. C., Baker, H. L., Jr., Houser, O. W., and Reese, D. F., 1974, *Radiology*, **111**, 709–715.

Ramachandran, G. N., and Lakshminarayanan, A. V., 1971, *Proc. Nat. Acad. Sci. U.S.*, **68**, 2236–2240.

Shepp, L. A., and Logan, B. F., 1974, *IEEE Trans. Nucl. Sci.*, **NS-21**(3), 21–43.